AIP | Applied Physics Letters

Continuous waves probing in dynamic acoustoelastic testing

M. Scalerandi, A. S. Gliozzi, M. Ait Ouarabi, and F. Boubenider

Citation: Applied Physics Letters **108**, 214103 (2016); doi: 10.1063/1.4952448
View online: http://dx.doi.org/10.1063/1.4952448
View Table of Contents: http://scitation.aip.org/content/aip/journal/apl/108/21?ver=pdfcov
Published by the AIP Publishing

Continuous waves probing in dynamic acoustoelastic testing

M. Scalerandi,[1] A. S. Gliozzi,[1] M. Ait Ouarabi,[1,2] and F. Boubenider[2]
[1]*Department of Applied Science and Technology, Condensed Matter and Complex Systems Physics Institute, Politecnico di Torino, Torino, Italy*
[2]*Laboratoire de Physique des Matériaux, Université des Sciences et de la Technologie Houari Boumediene, BP 32 El Alia, 16111 Bab Ezzouar, Alger, Algérie*

(Received 23 February 2016; accepted 12 May 2016; published online 26 May 2016)

Consolidated granular media display a peculiar nonlinear elastic behavior, which is normally analysed with dynamic ultrasonic testing exploiting the dependence on amplitude of different measurable quantities, such as the resonance frequency shift, the amount of harmonics generation, or the break of the superposition principle. However, dynamic testing allows measuring effects which are averaged over one (or more) cycles of the exciting perturbation. Dynamic acoustoelastic testing has been proposed to overcome this limitation and allow the determination of the real amplitude dependence of the modulus of the material. Here, we propose an implementation of the approach, in which the pulse probing waves are substituted by continuous waves. As a result, instead of measuring a time-of-flight as a function of the pump strain, we study the dependence of the resonance frequency on the strain amplitude, allowing to derive the same conclusions but with an easier to implement procedure. *Published by AIP Publishing.*
[http://dx.doi.org/10.1063/1.4952448]

Consolidated granular media display a complex nonlinear elastic response,[1–4] which derives from hysteresis in the stress-strain constitutive equation. This behavior, which includes memory effects,[1,5–8] relaxation phenomena,[9,10] nonlinear dependence of the modulus,[11,12] and attenuation coefficients[13,14] on the strain, etc., is also shared by damaged materials,[15–18] biological samples,[19,20] and metals with imperfect grain crystallisation.[21,22] Normally, the nonlinear hysteretic elastic behavior of various samples was analysed using dynamic techniques, which aim to evaluate the dependence of a measurable quantity on the strain. The nonlinear dependence of the modulus with increasing amplitude of excitation is reflected in a shift of the resonance frequency,[23,24] in the break of the superposition principle,[17,25] in the generation of higher order harmonics,[26,27] subharmonics[28,29] or sidebands,[30] and other observations. However, whatever the measured quantity is, its value depends on a sort of "average strain" supported by the sample during the experiment and this does not allow to directly extract the functional dependence of the elastic modulus on strain.

To have a direct measurement of the stress-strain relation without quasi-static testing and in the low tensile-compressive strain regime, the dynamic acoustoelastic testing (DAET) has been proposed.[31–35] The method is conceptually simple: a high amplitude and low frequency (LF) wave is used to excite continuously the sample (pump), while a high frequency (HF) pulse with small amplitude (probe) is used to measure the modulus, extracted from time-of-flight (TOF) measurements. If the probe is injected in the sample at different phases of the pump, it monitors the values of the elastic modulus at different strains, since the pulse propagates in a medium stressed by the wavefield due to the pump. The latter can be considered as quasistatic, being the period of the LF pump much larger than the TOF. The procedure is very efficient and reliable,[36,37] but needs a careful experimental implementation, an extensive post processing analysis, and a specific highly sensitive instrumentation.

The main issue for the realisation of a DAET experiment is the accurate measure of very small variations in the TOF. This is the same problem occurring in nonlinear dynamic measurements. In general, instead of measuring TOFs as a function of amplitude, it is easier to measure the resonance frequency as a function of amplitude, which, like TOFs, depends in a controllable way on the modulus. In this paper, we propose the same for the implementation of DAET. We will show that, replacing pulse probes with continuous waves probing, it is possible to extract the dependence on the strain of the resonance frequency and attenuation of the sample, with an easy to implement procedure. The proposed approach thus consists of an interaction of sine waves at and out of resonance, only similar to the nonlinear interaction of two resonant modes studied in Ref. 38 and to the interaction with torque modes reported in Ref. 39. In this paper, all measurements are expressed in volts, which could be transformed in strains if calibrated transducers, accelerometers, or laser vibrometers could be used for detection. From previous experience, where approximate calibration of the used sensors was performed, the strain corresponding to the voltages detected is in the range 10^{-8}–10^{-6}.

The method discussed in the following (continuous waves DAET: CW-DAET) has been implemented using a simple experimental setup. A Berea sandstone sample in the shape of a cylinder (1 cm diameter and 15 cm length) was available. It was equipped with two identical narrowband transducers glued with linear coupling (phenyl salicylate) on the bases of the cylinder, acting as emitter and receiver. Transducers had a diameter of 2 cm and a central frequency of 55.5 kHz. The emitting transducer was connected to an arbitrary waveform generator (Agilent 33500B) through a 20× linear amplifier (FLC Electronics A400). The receiving transducer was connected to an oscilloscope (Agilent Infiniium DSO9024H) for data acquisition. Resolution was set to 13 bit and sampling rate to 100 MSa/s. Signals were

recorded in a 50 ms time window once standing wave conditions were reached. The linearity of the experimental setup was carefully tested in the range of amplitudes adopted.

The method proposed here consists in injecting from the source transducer the sum of two sinusoidal waves (pump and probe):

$$u(t) = A_{LF} \sin 2\pi\omega_{LF}t + A_{HF} \sin 2\pi\omega_{HF}t. \quad (1)$$

The low frequency is chosen close to the first longitudinal resonance of the sample (compressional mode along the axes of the cylindrical sample), in order to optimise the pump strain distribution and amplitude. In our case, $\omega_{LF} = 9.4$ kHz. The low amplitude probing is performed in successive experiments sweeping the high frequency around a higher resonance mode of the sample. In the case considered, we choose $245\,\text{kHz} \leq \omega_{HF} \leq 255\,\text{kHz}$, with step $\Delta\omega = 0.2$ kHz. Also, we have chosen $A_{HF} = 0.5$ V and we have varied A_{LF} between 2 V and 18 V.

The detected signal could be filtered to obtain the response at low and high frequencies: see Figs. 1(a) and 1(b), where experimental results for $\omega_{HF} = 245$ kHz and $A_{LF} = 12$ V have been chosen. The high frequency response is modulated in amplitude (see Fig. 1(b)).

If we define a small time window (of duration corresponding to a few periods of the probing wave), we can move it along time. The choice of the window size should be as close as possible to the typical time-of-flight, so that, in the same time, the probe wave travels along the entire length of the cylindrical sample. In our case, experimental limitations in the choice of the low frequency pump wave (we had not the possibility to excite at lower frequency maintaining a significant strain excitation with the transducers at hand) forced the choice of a shorter window size (16 μs). The proportionality between voltage and strain perceived by the wave is maintained, although proper averaging on the strain distribution must be ensured for quantitative measurements.

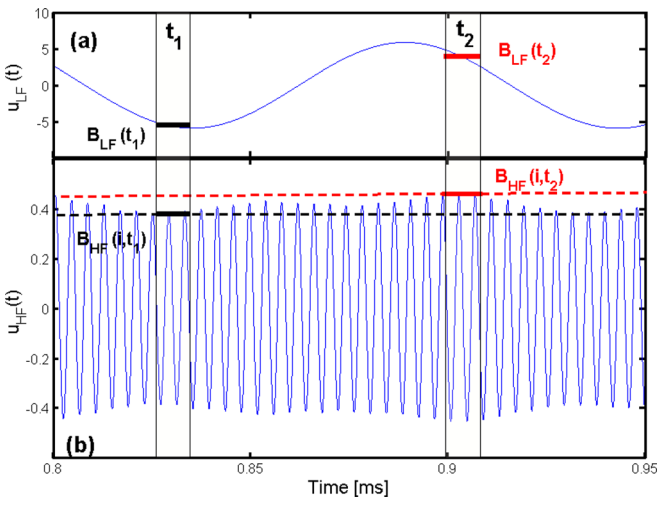

FIG. 1. Analysis of signals detected in the CW-DAET experiment: (a) signal filtered in the LF range; (b) signal filtered in the HF range. The grey rectangular area identifies portions of the signal at a given time and in a given time window which allow to calculate the average pump amplitude $B_{LF}(t)$ and the corresponding amplitude of the sine HF wave $B_{HF}(t)$. Bold solid lines identify these values, while dashed lines are a guide to the eyes to allow appreciating the modulation in amplitude of the HF wave.

In Fig. 1, we have shown the time window as a grey rectangle for two different times. For each position of the time window, we calculate the average value of the LF signal, which is almost constant in the chosen time interval. We term it $B_{LF}(t)$. In the same time window, we calculate the amplitude of the HF signal, which, being it composed of few cycles of a sinusoidal wave, corresponds to picking the maximum of the function in the interval. This quantity is termed $B_{HF}(t)$. This two quantities are identifiable with solid bold segments in Fig. 1. See the additional material for further details.[40]

Defining a frequency vector $\omega_{HF}(i)(i = 1...N)$ around the selected resonance frequency of the sample, we repeat the procedure by sweeping the frequency of the HF wave and we build a matrix of values $B_{HF}(i,t)$ and a vector $B_{LF}(t)$. It follows, eliminating the time variable, that the full information about the resonance structure is available in the form of a matrix $B_{HF}(i, B_{LF})$. Note that the construction of the matrix is mathematically simple, since measurements of the amplitudes of the two filtered signals are easy and accurate.

Selecting a row of the matrix B_{HF} (i.e., we fix t), we plot the amplitude of the probe signal as a function of frequency for an arbitrary value of the pump strain $B_{LF}(t)$, i.e., the resonance curve at a given strain. Typical results are shown in Figs. 2(a) and 2(b). In subplot (a), it could be easily noted an increase of the resonance frequency (resonance at which maximum in amplitude occurs) and of attenuation when the LF

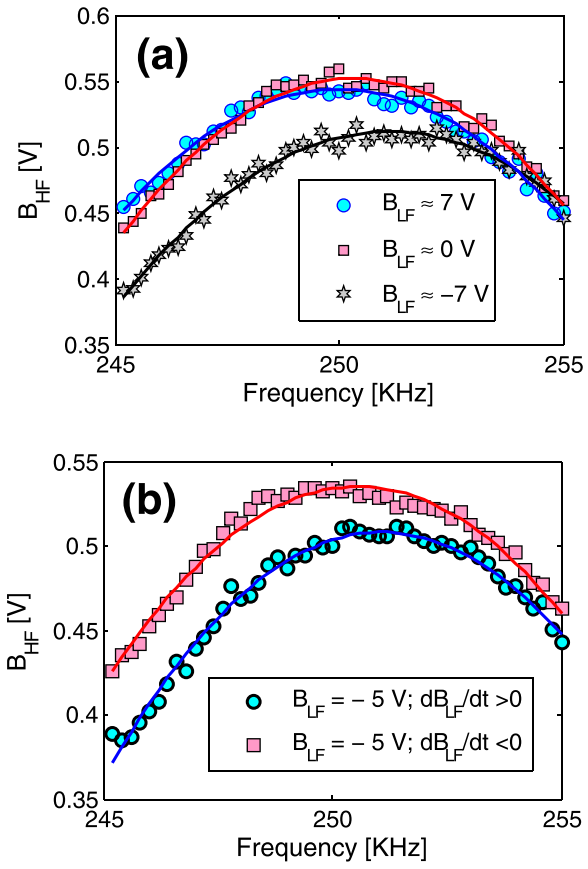

FIG. 2. Resonance frequency curves for different values of the pump strain B_{LF}. (a) Curves for varying amplitude of the strain; (b) curves for $B_{LF} = -5$ V measured when the strain derivatives are positive/negative (increasing/decreasing strain). Solid lines represent a quadratic fitting of the curves. Data refer to the experiment performed at the highest pump strain ($A_{LF} = 18$ V). Similar results are found when experiments are done at each pump amplitude.

strain changes from positive to negative. The resonance frequency $\omega_r(B_{LF})$ and resonant amplitude $\gamma_r(B_{LF})$ can be determined using a quadratic fitting. For every value of the LF strain, we have two resonance curves as shown in Fig. 2(b): one for increasing and one for decreasing strains, i.e., for different signs of the time derivative of B_{LF} with respect to time. Hysteresis is manifested, since the resonance frequency and amplitude differ significantly in the two branches.

Results of the analysis on the Berea sandstone sample are summarised in Fig. 3. The presence of hysteretic loops is clearly manifested. Also an offset (in both amplitude and frequency) is noticed, as shown by the downshift with increasing the range of variation of the pump strain (increasing the amplitude A_{LF} from the source). Conditioning is normally defined as the variation of the resonance amplitude and frequency when the pump strain is zero ($B_{LF}=0$). Results are qualitatively similar to those observed for other Berea sandstone samples using the standard DAET approach.[32,37] Note that the maximum variation in the resonance frequency is less than 1.5 kHz (i.e., less than 0.4%), while the variation in the amplitude at resonance is almost of 30%. Dominance of attenuation effects was also observed by other authors.[32,41] The resonance frequency change contains the same information as a TOF change, as measured in standard DAET, being the link between the resonance frequency and the wave speed linear as the link between TOF and velocity.

Following the same approach used by other authors,[31–33] the curves reported in Fig. 3 could be fitted with a parabolic approximation in the form

$$y = \alpha + \beta x + \delta x^2. \tag{2}$$

Albeit the fit is only a rough approximation of the data set, the three parameters give a quantitative representation of the offset, slope, and curvature of the curves (see the supplementary material for further details[40]). Eventually, the upgoing and downgoing branches of the curve could be fitted independently, to obtain a better description of the observed loops. The parameters of the fit are reported in Fig. 4 as a function of the pump amplitude.

In agreement with other observations, we notice that the result of the fit of both branches (blue symbols) is almost the average of the results of the fits performed considering separately the upgoing and downgoing branches (red and green symbols). For what concerns the offset (parameter α), we observe almost no difference in the three fits (total, upgoing only, downgoing only), indicating that the hysteretic loops of Fig. 3 show two branches which intersect approximately at zero amplitude of the pump. For the global fit results (blue symbols), we notice that the curvature (parameter δ) decreases in modulus with increasing strain (pump amplitude), while slope (parameter β) is only slightly dependent on the maximum strain, for both resonance amplitude and resonance frequency curves. A stronger dependence on the pump amplitude is found when the upgoing and downgoing branches of the curves are fitted independently.

Finally, we have applied the CW-DAET approach to estimate nonlinearity in different materials, as shown in Fig. 5, where the variation in the resonance frequency and the resonance amplitude are reported vs. the pump amplitude. In the case of PMMA (first row), only a slight shift in the resonance frequency (left column) and no dependence of the resonance amplitude on strain (right column) are observed. The absence of hysteretic loops and memory is the indication that, as expected, only classical nonlinearity is relevant. Note that nonlinear effects are very small. As already discussed, results for Berea sandstone (second row) are in agreement

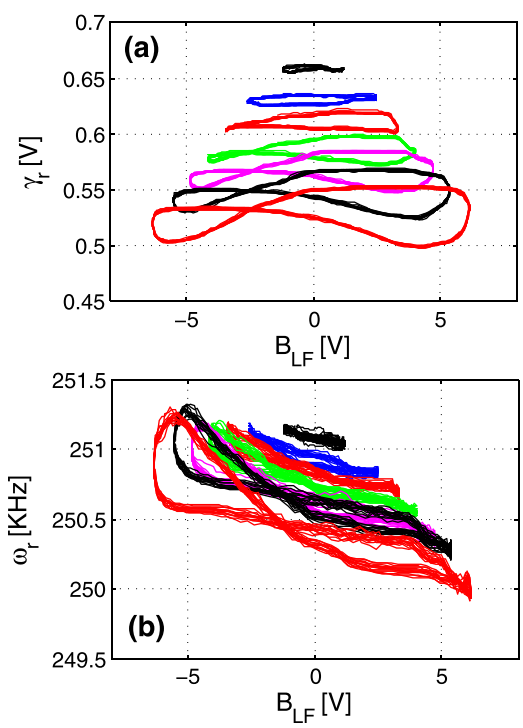

FIG. 3. Resonance amplitude γ_r and resonance frequency ω_r as a function of the strain amplitude induced by the pump.

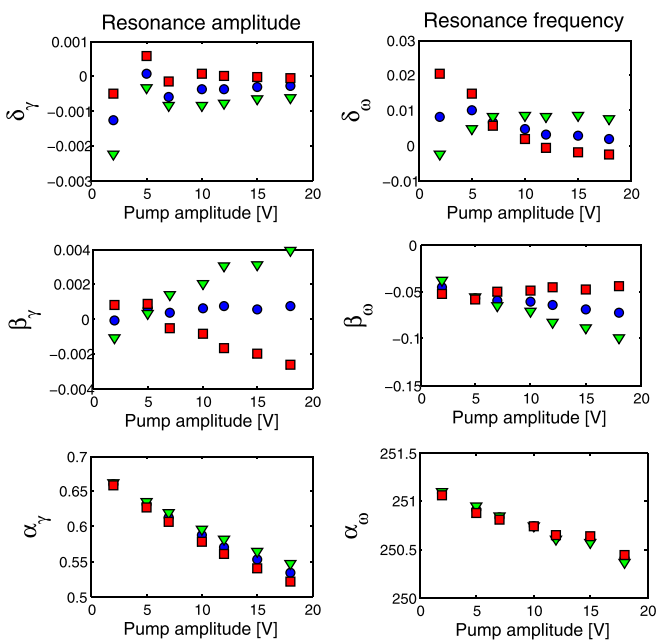

FIG. 4. Parameters describing curvature, slope, and offset of the curves reported in Fig. 3 vs. amplitude of the pump. For all the three parameters, red squares and green triangles correspond to the values of the parameters obtained fitting the upgoing and downgoing branches independently. Left column: parameters for the resonance amplitude. Right column: parameters for the resonance frequency.

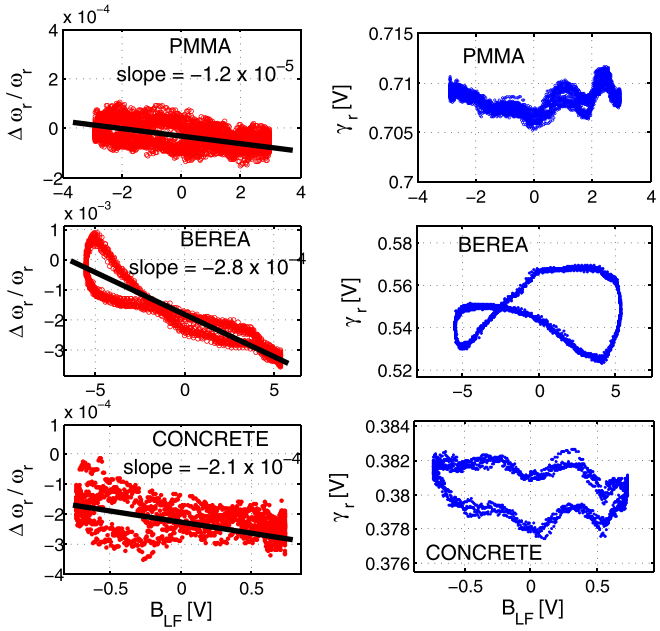

FIG. 5. Resonance frequency variation and resonance amplitude γ_r as a function of the strain amplitude induced by the pump for different materials. Solid lines in the left column correspond to a linear fit of the data, with the slopes reported in the figure.

with observations reported using standard DAET. Concrete (third row) exhibits only slight dependence of the resonance frequency on strain, with a significant hysteretic loop with elliptical shape for the resonance amplitude dependence. Memory is also observed. The result is in qualitative agreement with observations reported using standard DAET.[42] We have also estimated the slopes of the resonance vs. strain curves (reported in Fig. 5). It is noticeable that the ratio between slopes for Berea and PMMA is about 23, in agreement with the ratio between the β coefficients experimentally estimated for Berea ($\beta_B \approx 200$ (Ref. 32)) and for PMMA ($\beta_P \approx 8$ (Ref. 43)).

In this contribution, we have presented a variation in the dynamic acoustoelastic testing method, in which pulse probing is substituted with continuous waves probing. Our experimental setup was not optimised. In particular, the lowest the pump frequency, the better the measurement since longer time windows of HF signals could be used. Nevertheless, results shown here are in excellent qualitative agreement with expectations for classical (PMMA) and nonclassical (Berea and concrete) test samples. To be implemented, the approach requires strong attenuation and an accurate analysis of the modes for quantification. The advantage with respect to DAET is the ease of implementation and post processing-analysis.

[1]R. A. Guyer, J. Tencate, and P. A. Johnson, Phys. Rev. Lett. **82**, 3280–3283 (1999).
[2]P. A. Johnson and A. Sutin, J. Acoust. Soc. Am. **117**, 124–130 (2005).
[3]G. Renaud, J. Riviere, S. Haupert, and P. Laugier, J. Acoust. Soc. Am. **133**, 3706–3718 (2013).
[4]P. Antonaci, C. L. E. Bruno, P. G. Bocca, M. Scalerandi, and A. S. Gliozzi, Cem. Concr. Res. **40**, 340–346 (2010).
[5]J. A. TenCate, D. Pasqualini, S. Habib, K. Heitmann, D. Higdon, and P. A. Johnson, Phys. Rev. Lett. **93**, 065501 (2004).
[6]T. J. Ulrich and T. W. Darling, Geophys. Res. Lett. **28**, 2293–2296, doi:10.1029/2000GL012480 (2001).
[7]K. C. E. Haller and C. M. Hedberg, Phys. Rev. Lett. **100**, 068501 (2008).
[8]M. Scalerandi, A. S. Gliozzi, C. L. E. Bruno, and P. Antonaci, Phys. Rev. B **81**, 104114 (2010).
[9]J. A. TenCate, E. Smith, and R. A. Guyer, Phys. Rev. Lett. **85**, 1020 (2000).
[10]M. Bentahar, H. El Aqra, R. El Guerjouma, M. Griffa, and M. Scalerandi, Phys. Rev. B **73**, 014116 (2006).
[11]G. Renaud, S. Calle, J.-P. Remenieras, and M. Defontaine, IEEE Trans. Ultrason. Ferroelectr. Freq. Control **55**, 1497–1507 (2008).
[12]C. Pecorari, Proc. R. Soc. A **471**, 20150369 (2015).
[13]P. Finkel, A. G. Zhou, S. Basu, O. Yeheskel, and M. W. Barsoum, Appl. Phys. Lett. **94**, 241904 (2009).
[14]C. Trarieux, S. Calle, H. Moreschi, G. Renaud, and M. Defontaine, Appl. Phys. Lett. **105**, 264103 (2014).
[15]I. Solodov and G. Busse, Appl. Phys. Lett. **102**, 061905 (2013).
[16]C. Campos-Pozuelo, C. Vanhille, and J.-A. Gallego-Juarez, IEEE Trans. Ultrason. Ferroelectr. Freq. Control **53**, 175–184 (2006).
[17]M. Scalerandi, M. Griffa, P. Antonaci, M. Wyrzykowski, and P. Lura, J. Appl. Phys. **113**, 154902 (2013).
[18]F. Ciampa, E. Onder, E. Barbieri, and M. Meo, J. Nondestr. Eval. **33**, 515–521 (2014).
[19]S. Haupert, S. Guerard, F. Peyrin, D. Mitton, and P. Laugier, PLoS One **9**, e83599 (2014).
[20]M. Muller, A. Sutin, R. Guyer, M. Talmant, P. Laugier, and P. A. Johnson, J. Acoust. Soc. Am. **118**, 3946–3952 (2005).
[21]J. H. Cantrell, J. Appl. Phys. **106**, 093516 (2009).
[22]M. Scalerandi, A. S. Gliozzi, and D. Olivero, J. Nondestr. Eval. **33**, 269–278 (2014).
[23]Y. Baccouche, M. Bentahar, C. Mechri, R. El Guerjouma, and M. H. Ben Ghozlen, J. Acoust. Soc. Am. **133**, EL256–EL261 (2013).
[24]J. Chen, J. Y. Kim, K. E. Kurtis, and L. J. Jacobs, J. Acoust. Soc. Am. **130**, 2728–2737 (2011).
[25]M. Scalerandi, A. S. Gliozzi, C. L. E. Bruno, D. Masera, and P. Bocca, Appl. Phys. Lett. **92**, 101912 (2008).
[26]C. Payan, V. Garnier, J. Moysan, and P. A. Johnson, J. Acoust. Soc. Am. **121**, EL125 (2007).
[27]K. Van den Abeele and J. De Visscher, Cem. Concr. Res. **30**, 1453–1464 (2000).
[28]I. Solodov, J. Wackerl, K. Pfleiderer, and G. Busse, Appl. Phys. Lett. **84**, 5386–5388 (2004).
[29]Y. Ohara, T. Mihara, R. Sasaki, T. Ogata, S. Yamamoto, Y. Kishimoto, and K. Yamanaka, Appl. Phys. Lett. **90**, 011902 (2007).
[30]K. Van den Abeele, W. Desadeleer, G. De Schutter, and M. Wevers, Cem. Concr. Res. **39**, 426–432 (2009).
[31]G. Renaud, S. Calle, and M. Defontaine, Appl. Phys. Lett. **94**, 011905 (2009).
[32]G. Renaud, P.-Y. Le Bas, and P. A. Johnson, J. Geophys. Res. **117**, B06202, doi:10.1029/2011JB009127 (2012).
[33]S. Haupert, J. Riviere, B. E. Anderson, Y. Ohara, T. J. Ulrich, and P. Johnson, J. Nondestr. Eval. **33**, 226–248 (2014).
[34]F. Moradi-Marani, S. A. Kodjo, P. Rivard, and C. P. Lamarche, J. Nondestr. Eval. **33**, 288–298 (2014).
[35]T. Gallot, A. Malcolm, T. L. Szabo, S. Brown, D. Burns, and M. Fehler, J. Appl. Phys. **117**, 034902 (2015).
[36]M. Scalerandi, A. S. Gliozzi, S. Haupert, G. Renaud, M. Ait Ouarabi, and F. Boubenider, J. Appl. Phys. **118**, 124905 (2015).
[37]J. Rivière, G. Renaud, R. A. Guyer, and P. A. Johnson, J. Appl. Phys. **114**, 054905 (2013).
[38]V. E. Nazarov, Acoust. Phys. **53**, 217 (2007).
[39]J. Birch, J. Appl. Phys. **8**, 129 (1937).
[40]See supplementary material at http://dx.doi.org/10.1063/1.4952448 for the description of this aspect.
[41]S. Haupert, G. Renaud, J. Riviere, M. Talmant, P. A. Johnson, and P. Laugier, J. Acoust. Soc. Am. **130**, 2654–2661 (2011).
[42]J. N. Eiras, Q. A. Vu, M. Lott, J. Pay, V. Garnier, and C. Payan, Ultrasonics **69**, 29–37 (2016).
[43]M.-C. Wu and W. P. Winfree, in *Proceedings of the IEEE 1989 Ultrasonic Symposium*, edited by B. R. McAvoy (IEEE, New York, 1989), pp. 1241–1244.